

## **Spatial Discretization of Strain Localization**

E. Rizzi<sup>1</sup> and K. Willam

*University of Colorado Boulder, CEAE Dept., Boulder, USA*

<sup>1</sup>*On leave from Politecnico di Milano, DIS, Milano, Italy*

### ABSTRACT

In recent years novel finite element techniques have been developed for capturing strain localization. Their objective is to minimize mesh sensitivity of numerical solutions in the presence of destabilizing material effects due to stiffness degradation, strength softening and loss of associativity. In the context of localization analysis two computational features are examined to study the effect of arc-length control and of enhanced finite elements in the form of the incompatible QM6-element. This element formulation captures discontinuities due to strain localization and thus reduces mesh locking due to directional bias.

### INTRODUCTION

Strain localization is normally associated with the formation of spatial discontinuities which entail jumps in the velocity gradient and consequently also in the strain rate (see Rizzi [10]). The underlying mode of discontinuous bifurcation is characterized by the unit vector normal to the discontinuity surface and the unit vector which defines the localized motion. Thereby the critical localization mode is a functional of the state of stress and of the underlying tangential constitutive description of elastic damage and/or elastoplastic softening.

On one hand localization initiates at the constitutive level, whereby the onset of discontinuous bifurcation is indicated by a zero eigenvalue of the localization tensor, while the corresponding eigenvector characterizes the mode of bifurcation (Borré and Maier [2], Ottosen and Runesson [7], Bigoni and Hueckel [1], Rizzi [10]). On the other hand, localization emerges at the structural level within the framework of progressive failure analysis which requires solution of hard nonlinearities in the form of spatial discontinuities and strong path-dependence. Localization analysis at the constitutive level provides additional information which should be used to guide the failure simulation on the structural level and to reduce mesh sensitivity due to spatial finite element discretization (Ortiz et al. [6], Steinmann and Willam [13], Larsson and Runesson [5]). In the presence of strain localization, progressive failure requires additional regularization of the

post-bifurcation response in order to ensure mesh-objectivity, i.e. failure predictions which are independent of mesh orientation and mesh density (see de Borst [4] for a concise treatment of this phenomenon). Regularization can be achieved at the constitutive level by introducing enriched material descriptions which prevent localization altogether (see Willam and Dietsche [15] for a comprehensive review of regularization strategies). Alternatively, the energy dissipation may be controlled in the post-bifurcation response regime with the aid of an intrinsic length scale (Larsson and Runesson [5]). If the emerging failure mode is to be captured correctly, appropriate finite element strategies must be developed, either by alignment of standard displacement elements along the failure band (Larsson and Runesson [5]), or by enhancement of the eigenspace of the finite element approximation (Ortiz et al. [6], Steinmann and Willam [13]).

This contribution will illustrate the effect of two computational features on progressive failure simulations of the axial extension test problem. To this end a research-oriented finite element code was extended to accommodate in the classical arc-length technique by Wempner [14] and Riks [9] in the form of the arc-length adaptation by Crisfield [3]. A simple back-tracking strategy was incorporated in order to capture the post-peak and snap-back response behavior beyond the limit/bifurcation point. As a second feature the enriched QM6 finite element by Wilson and Taylor was used in the mixed variational format advocated by Simo and Rifai [12] which was analyzed by Steinmann and Willam [13] in the context of localization analysis. The use of the QM6-element captures formation of inclined shear bands which are in close agreement with the analytical predictions of discontinuous bifurcation at the constitutive level. The regularization of post-bifurcation behavior will be addressed in a sequel to this paper.

## STRAIN LOCALIZATION CONDITIONS

Strain localization is synonymous with the formation of weak discontinuities, i.e. jumps of the strain rather than the displacement field across a discontinuity surface. Consequently, at the onset of bifurcation the displacement rate remains continuous, while the rate of the displacement gradients exhibits jumps across the discontinuity surface which separates the continuum into two regions on the ‘+’ and ‘-’ side of the discontinuity surface:

$$[[\dot{\mathbf{u}}]] = \dot{\mathbf{u}}^+ - \dot{\mathbf{u}}^- = \mathbf{0} \quad ; \quad [[\nabla\dot{\mathbf{u}}]] = \nabla\dot{\mathbf{u}}^+ - \nabla\dot{\mathbf{u}}^- \neq \mathbf{0} \quad (1)$$

The jump in the displacement gradient must satisfy Maxwell’s compatibility conditions  $[[\nabla\dot{\mathbf{u}}]] = \dot{\gamma}\mathbf{M} \otimes \mathbf{N}$ , a topic which was examined in detail by Rizzi [10] with a summary of related references. In the Maxwell’s relation  $\dot{\gamma}$  denotes the amplitude of the jump,  $\mathbf{N}$  the unit vector normal to the discontinuity surface, and  $\mathbf{M}$  the unit vector which characterizes the localization motion. Mode I failure occurs when  $\mathbf{M} \parallel \mathbf{N}$ , and mode II failure when  $\mathbf{M} \perp \mathbf{N}$ , while all other angles indicate mixed mode localization.

Equilibrium of surface tractions requires that the traction vector  $\dot{\mathbf{t}}_N = \mathbf{N} \cdot \dot{\boldsymbol{\sigma}}$  remains continuous and does not exhibit jumps, i.e.  $[[\dot{\mathbf{t}}_N]] = 0$ . Considering constitutive rate relations in the differential format  $\dot{\boldsymbol{\sigma}} = \mathbf{E}_t : \boldsymbol{\epsilon}$ , the combination

of both kinematic and static conditions across the discontinuity surface leads to the localization condition  $\mathbf{Q}_t \cdot \mathbf{M} = \mathbf{0}$ , where  $\mathbf{Q}_t$  defines the tangent localization tensor as

$$\mathbf{Q}_t = \mathbf{N} \cdot \mathbf{E}_t \cdot \mathbf{N} \quad (2)$$

According to this notation  $\mathbf{M}$  denotes the critical eigenvector which characterizes the mode of localization associated with the vanishing eigenvalue of  $\mathbf{Q}_t$ . The localization condition may be expressed in terms of the determinant  $\det(\mathbf{Q}_t) = 0$  (Borré and Maier [2]) which is normalized in Fig. 1(a) by the corresponding value of the elastic operator to plot its variation as a function of all possible localization directions. Alternatively the localization condition may be expressed in terms of the maximum hardening/softening modulus  $H_{cr}$  which is required for discontinuous bifurcation in a given direction  $\mathbf{N}$ . The onset of localization is indicated by the critical localization direction which maximizes the critical hardening parameter  $H_{loc} = H_{cr}^{max}$ , see Fig. 1(b).

The localization condition was studied analytically in the context of bifurcation analysis of elastoplastic solids (Ottosen and Runesson [7]), and for elastic degradation (Bigoni and Hueckel [1], Rizzi [10]). Fig. 1 summarizes the localization results for  $J_2$ -plasticity and scalar damage for loading in axial extension (3D/plane strain analysis taken from Rizzi [10]). Fig. 1(a) depicts the variation of the normalized localization indicator  $\mu = \det(\mathbf{Q}_{ep})/\det(\mathbf{Q}_e)$  as a function of all possible localization directions  $0^\circ \leq \theta \leq 180^\circ$  assuming perfect elastoplastic behavior. The minima depend on the Poisson's ratio  $\nu$ , indicating that in plane strain considerable softening is required for localization to occur. Fig. 1(b) illustrates the localization condition in terms of the maximum hardening modulus  $H_{cr}$  for the  $(1-D)$  scalar damage model. The differences of the critical localization directions show strong dependence on Poisson's ratio. In particular, for  $\nu = 0.3$ , elastoplasticity predicts an angle of discontinuity  $\theta_{cr} = 41.17^\circ$  between the loading axis and the normal  $\mathbf{N}$  to the shear band, whereas the scalar format of elastic damage results in  $\theta_{cr} = 33.21^\circ$ .

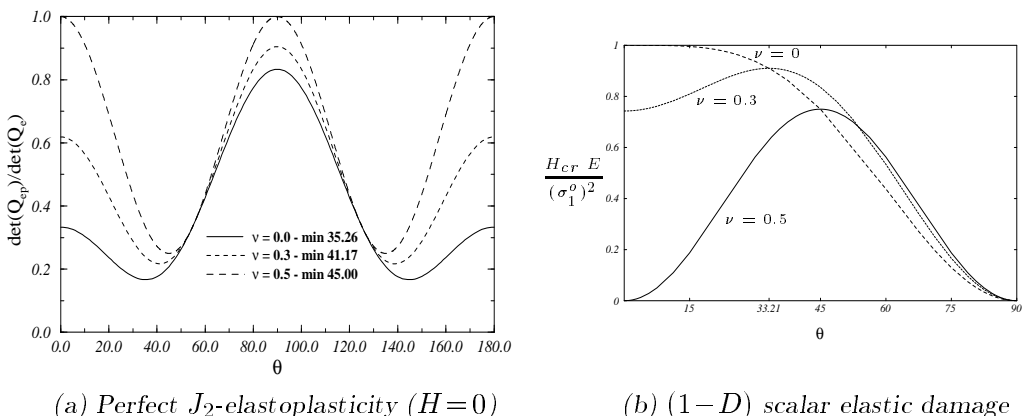


Figure 1: Analytic conditions for localization in axial extension.

## COMPUTATIONAL STRATEGIES FOR THE POST-PEAK REGIME

In the presence of strain localization, i.e. when the assumed material law and the local state of internal variables result in spatial bifurcation, additional techniques are required to monitor the numerical solution. First, an indirect force-displacement control must be introduced to overcome limit points and snap-back points. The classical arc-length approach by Wempner [14] and Riks [9] with the arc-length adaptation by Crisfield [3] combined with a simple back-tracking strategy captures fairly sharp snap-backs in the case of a brittle failure descriptions when the traditional (1- $D$ ) damage model is used, see Simo and Ju [11]. Second, the incompatible QM6-element by Wilson and Taylor and its generalization by Simo and Rifai [12] captures localization according to the ‘‘Weak Localization Test’’ by Steinmann and Willam [13], and thus should be capable to describe shear-bands without mesh re-alignment.

### Arc-length control

For the analysis of the post-peak and snap-back regimes the classical arc-length control is imperative which was originally proposed by Wempner [14] and Riks [9]. In that approach the trial solution  $\Delta \mathbf{u}_t$  in the displacement vector/load parameter plane  $(\mathbf{u}, \lambda)$  is embedded in the tangent plane, while its correction is searched along a path perpendicular to the tangent. The final increment  $\Delta \mathbf{u}$  must then satisfy the constraint equation

$$\Delta \mathbf{u} \cdot \Delta \mathbf{u} + (\Delta \lambda)^2 = (\Delta s)^2 \quad (3)$$

where  $\Delta s$  indicates the arc-length in that plane. Since the displacement norm uses all the components of the displacement vector, a better but problem dependent approach extracts the dominant degrees of freedom in the case of highly localized deformation patterns (de Borst [4]).

The sparsity of the tangent stiffness matrix  $\mathbf{K}_t$  can be maintained by decomposing the displacement increment into two contributions  $\Delta \mathbf{u} = \Delta \lambda \Delta \mathbf{u}_1 + \Delta \mathbf{u}_2$  and by solving two decoupled algebraic systems (Ramm [8], de Borst [4])

$$\mathbf{K}_t \cdot \Delta \mathbf{u}_1 = \mathbf{P} ; \quad \mathbf{K}_t \cdot \Delta \mathbf{u}_2 = \mathbf{R} \quad (4)$$

where  $\mathbf{P}$  denotes the load vector and  $\mathbf{R}$  the out-of-balance force vector (Ramm [8]).

Automatic arc-length adjustment is necessary for accelerating the convergence and for stabilizing the number of iterations. A simple strategy along the line of the backtracking algorithm with trust regions for numerical unconstrained optimization problems decreases the step size for achieving convergence near limit points. They are detected by negative diagonal elements of the stiffness matrix during pivoting:

$$\Delta s \leftarrow \Delta s / \alpha \quad \text{with } 1 \leq \alpha \leq 2 \quad (5)$$

where  $\alpha$  is conveniently chosen after a preliminary calculation. The arc-length might decrease dramatically near the limit point. An adaptive control of the number of iterations for each step allows to vary the step size such that the number of iteration remains at the optimal value  $n^{opt}=4 \div 5$

$$\text{Crisfield [3]} : \Delta s \leftarrow \Delta s (n^{opt}/n_{prev}) \quad \text{Ramm [8]} : \Delta s \leftarrow \Delta s \sqrt{(n^{opt}/n_{prev})} \quad (6)$$

The arc-length adjustment by Crisfield [3] performed better and stabilized the number of iterations after each perturbation. Furthermore, upper and lower bounds on the arc-length were established to assure accuracy and economy of the numerical solution.

#### The QM6-Element

The incompatible QM6-element was originally formulated by Wilson and Taylor (see Steinmann and Willam [13] for application to localization analysis) with the purpose of enhancing the bending performance of the standard bilinear quadrilateral Q4-element. The four additional quadratic terms in the displacement expansion, which are expressed in terms of normalized coordinates  $\xi$ ,  $\eta$ , are introduced to reduce shear locking.

$$u = N_i u_i + (1 - \xi^2) d_9 + (1 - \eta^2) d_{10}; \quad v = N_i v_i + (1 - \xi^2) d_{11} + (1 - \eta^2) d_{12} \quad (7)$$

This enhancement leads to a uniform state of shear strain within the element domain, while the direct strain components form a set of complete linear polynomials. The original formulation was generalized by Simo and Rifai [12] in terms of a mixed variational principle, in which the augmented strain  $\tilde{\boldsymbol{\epsilon}} = \boldsymbol{\epsilon} - \nabla_s \mathbf{u}$  was expressed as  $\tilde{\boldsymbol{\epsilon}} = \mathbf{B}_2 \cdot \tilde{\mathbf{d}}$ , where

$$\mathbf{B}_2 = \begin{bmatrix} \xi & 0 & 0 & 0 \\ 0 & \eta & 0 & 0 \\ 0 & 0 & \xi & \eta \end{bmatrix}; \quad \boldsymbol{\epsilon} \rightarrow \begin{bmatrix} 1 & 0 & 0 & \xi & \eta & 0 & 0 \\ 0 & 1 & 0 & 0 & 0 & \xi & \eta \\ 0 & 0 & 1 & 0 & 0 & 0 & 0 \end{bmatrix} \quad (8)$$

This element satisfies the ‘‘Weak Localization Test’’ proposed by Steinmann and Willam [13] to verify whether an element is able to capture a weak discontinuity at the element level. According to this test the QM6-element should perform well without introducing directional bias, thus no alignment of the mesh should be required along the shear bands.

## AXIAL EXTENSION PROBLEM

The two computational strategies are used to study the formation of shear bands in axial extension. A rectangular specimen with the aspect ratio  $a/b = 1/2$  is considered under plane strain. Different mesh discretizations are used to examine their effect on idealizations of the entire specimen and of a quarter subdomain using double symmetry. The uniform state of stress and strain is perturbed in order to induce localization. Two imperfections are considered, (i) a geometric imperfection consisting of a small coordinate perturbation at a boundary node, and (ii) lateral constraints at the two end surfaces which simulate the lateral confinement of the rigid loading platens.

To compare elastic damage and softening plasticity descriptions two material models are considered: (a) the  $(1-D)$  scalar damage model which was proposed by Simo and Ju [11] is based on the evolution law  $D = 1 - (1-A) \bar{\tau}_o / \bar{\tau} - A e^{B(\bar{\tau}_o - \bar{\tau})}$ , where  $\bar{\tau} = \sqrt{\boldsymbol{\epsilon} : \mathbf{E}_o : \boldsymbol{\epsilon}}$ , and where  $\mathbf{E}_o$  denotes the initial stiffness with  $E_o = 30,000$  *ksi*,  $\nu = 0.3$ ,  $A = 0.6$ ,  $B = 2$  *in*/ $\sqrt{kip}$ ,  $\bar{\tau}_o = 0.01$   $\sqrt{kip}$ /*in*. (b) the Huber-Mises plasticity model which is based on bilinear hardening/softening uses the same elastic moduli while  $\sigma_y = 36$  *ksi* defines the yield limit in axial tension/compression.

The load-displacement diagrams are shown in Fig. 2 for the case of scalar damage. The effect of the two alternative perturbations are compared together with the two quadrilateral finite element formulations. Note the appearance of sharp snap-back which are captured only by the highly refined mesh layouts.

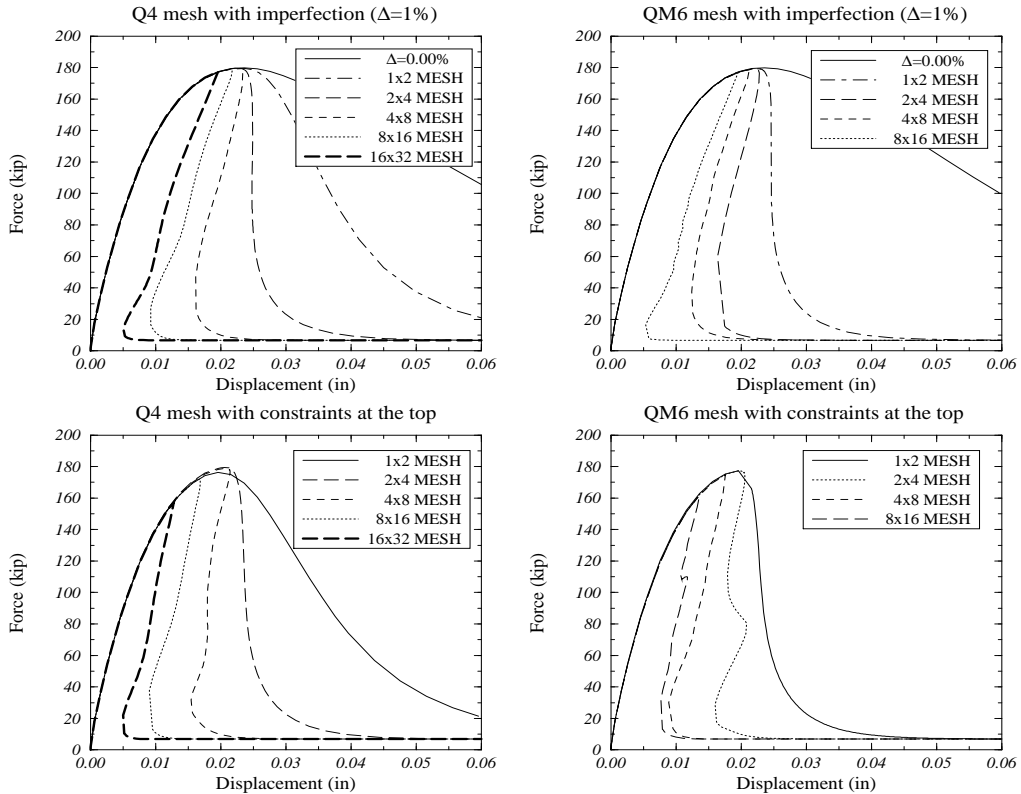


Figure 2: Axial extension problem of the elastic scalar damage specimen.

The capabilities of the QM6 elements are shown in Fig. 3, where the inclined shear band forms at  $45^\circ$  in the case of the Huber-Mises material with softening ( $H=500 \text{ ksi}$ ). This is in good agreement with the analytical prediction shown in Fig. 1. The uniform deformation state is altered by the lateral constraints of the loading platens. Fig. 3 compares the effects of (16x32) discretization of the quarter specimen with those of the entire specimen. It also depicts the results of the traditional Q4-element and those of the enhanced QM6-element. The symmetry constraint remains insignificant with respect to shear banding since discretization of the entire specimen leads to the same failure pattern as the quarter idealization. Separate computations with different aspect ratios of the rectangular specimen shows that the  $45^\circ$  orientation is not biased by the particular  $a/b = 1/2$ -ratio. It is interesting to note that the elastoplastic shear band orientation is fairly independent of the variation of  $\nu$ , while the scalar damage material description results in an inclined shear band only for  $\nu \rightarrow 0.5$ . In all other cases localization appears always in a single row of elements transverse to the load direction indicating mode I type failure, which should emerge only for  $\nu \rightarrow 0$  according to Fig. 1(b). This seems to be due to the absence of irreversible strains which trigger the incompressible mode of plastic bifurcation.

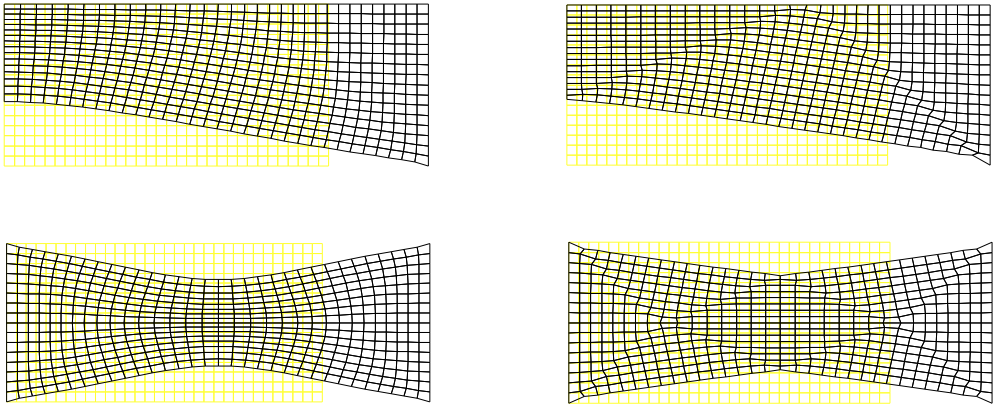


Figure 3: Comparison of Q4-(left) and QM6-(right) discretizations using 16x32 FE.

The effect of different locations of the geometric imperfection on the formation of shear-bands is shown in Fig. 4. The geometric imperfections are sequentially placed at the four corners of the rectangular specimen. The deformed meshes are plotted with different amplification factors, which vary from 25 to 100.

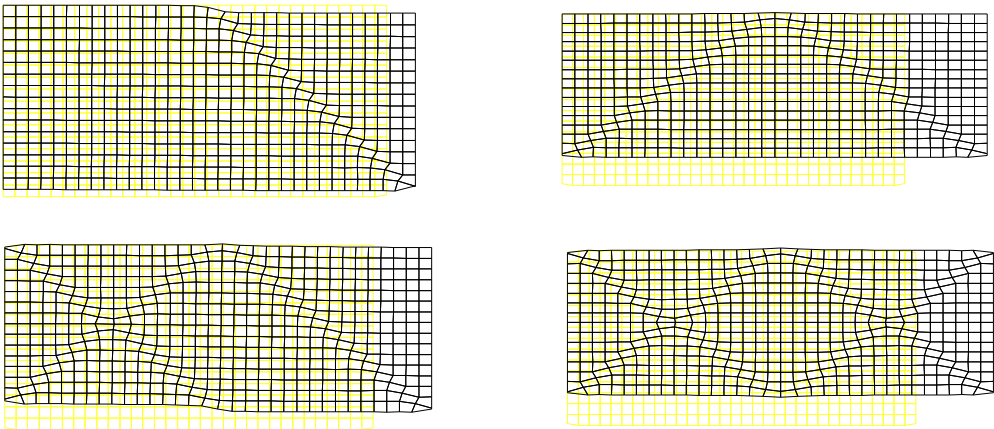


Figure 4: Discretization of entire specimen: effect of different geometric imperfections.

## CONCLUSIONS

The arc-length control together with the enhanced QM6-element show promise for the solution of boundary value problems which exhibit localization. Regularization with respect to the directional properties of the mesh layout is accomplished by the enhanced quadrilateral element, although this should be verified with additional realistic engineering problems. Regularization with respect to mesh densification will be considered in a sequel of this paper.

## ACKNOWLEDGMENTS

The authors thank the US National Science Foundation, NSF, for the financial support under grant MSS-9103589 at the University of Colorado - Boulder. The first author also thanks the Italian Ministry of University, Scientific and Technological Research for its financial assistance.

## REFERENCES

- [1] Bigoni, D., and Hueckel, T. "Uniqueness and localization-II. Coupled elastoplasticity", *I. J. Sol. Struct.*, 28 (2), 215-224, 1991.
- [2] Borré, G., and Maier, G. "On linear versus nonlinear flow rules in strain localization analysis", *Meccanica*, 24, 36-41, 1989.
- [3] Crisfield, M.A. "A fast incremental/iterative solution procedure that handles snap-through", *Comp. Struct.*, 13, 55-62, 1981.
- [4] de Borst, R. "Computation of post-bifurcation and post-failure behavior of strain-softening solids", *Comp. Struct.*, 25(2), 211-224, 1987.
- [5] Larsson, R. and Runesson, K. "Discontinuous displacement approximation for capturing plastic localization", *I. J. Num. Meth. Eng.*, 36, 2087-2105, 1993.
- [6] Ortiz, M., Leroy, Y. and Needleman, A. "A finite element method for localized failure analysis", *Comp. Meth. Appl. Mech. Eng.*, 61, 189-214, 1987.
- [7] Ottosen, N. S., and Runesson, K. "Properties of discontinuous bifurcation solutions in elasto-plasticity", *I. J. Sol. Struct.*, 27(4), 401-421, 1991.
- [8] Ramm, E. "Strategies for tracing the nonlinear response near limit points", *Proc. of Europe-US Workshop*, (Ed. Wunderlich, W., Stein, E. and Bathe, K.J.), 63-89, Ruhr-Universität Bochum, Germany, July 28-31, 1980, Springer-Verlag, 1981.
- [9] Riks, E. "An incremental approach to the solution of snapping and buckling problems", *I. J. Sol. Struct.*, 15, 529-551, 1979.
- [10] Rizzi, E. "Localization analysis of damaged materials", *Int. Rep. CU/SR-93/5*, CEAE Dept., University of Colorado, Boulder, U.S.A., 1993.
- [11] Simo, J. C., and Ju, J. W. "Strain- and stress-based continuum damage models - I. Formulation", *I. J. Sol. Struct.*, 23(7), 821-840, 1987.
- [12] Simo, J. C., and Rifai, M.S. "A class of mixed assumed strain methods and the method of incompatible modes", *I. J. Num. Meth. Engrg.*, 29, 1595-1638, 1990.
- [13] Steinmann, P. and Willam, K. "Performance of enhanced finite element formulations in localized failure computations", *Comp. Meth. Appl. Mech. Eng.*, 90, 845-867, 1991.
- [14] Wempner, G.A. "Discrete approximations related to nonlinear theories of solids", *I. J. Sol. Struct.*, 7, 1581-1599, 1971.
- [15] Willam, K. and Dietsche, A. "Regularization of localized failure computations", (Ed. Owen, D.R.J., Oñate, E. and Hinton, E.), 2185-2204, *Proc. of COMPLAS III, Part II*, Barcelona, Spain, April 6-10, 1992, Pineridge Press, Swansea, 1992.